Bioorganic Chemistry 114 (2021) 105112

Contents lists available at ScienceDirect

Bioorganic Chemistry

journal homepage: www.elsevier.com/locate/bioorg

Phenolic constituents isolated from *Senna tora* sprouts and their neuroprotective effects against glutamate-induced oxidative stress in HT22 and R28 cells

Jaeyoung Kwon [a,b,1], Hoseong Hwang [a,1], Baskar Selvaraj [a], Jung Hwan Lee [a], Woongbi Park [a], Seung Mok Ryu [c], Dongho Lee [d], Jin-Soo Park [a], Hyoung Seok Kim [a], Jae Wook Lee [a], Dae Sik Jang [e,*], Hak Cheol Kwon [a,*]

[a] KIST Gangneung Institute of Natural Products, Korea Institute of Science and Technology (KIST), Gangneung 25451, Republic of Korea
[b] Division of Bio-Medical Science & Technology, KIST School, University of Science and Technology (UST), Gangneung 25451, Republic of Korea
[c] Herbal Medicine Resources Research Center, Korea Institute of Oriental Medicine (KIOM), Naju 58245, Republic of Korea
[d] Department of Plant Biotechnology, College of Life Sciences and Biotechnology, Korea University, Seoul 02841, Republic of Korea
[e] Department of Life and Nanopharmaceutical Sciences, College of Pharmacy, Kyung Hee University, Seoul 02447, Republic of Korea

ARTICLE INFO

Keywords:
Sprout
Senna tora
Fabaceae
Naphthopyrone
Antioxidant
Neuroprotective effect

ABSTRACT

The consumption of sprouts has been steadily increasing due to their being an excellent source of nutrition. It is known that the bioactive constituents of legumes can be increased after germination. In this study, the extract from *Senna tora* sprouts is shown to exhibit improved radical scavenging activities and better neuroprotective effects in HT22 hippocampal neuronal (HT22) and R28 retina precursor (R28) cells than those from seeds due to an increased content of phenolic constituents, especially compounds **1** and **3**–**6**. A phytochemical investigation of *S. tora* sprouts resulted in the isolation of two new naphthopyrone glycosides (**1**–**2**) with 27 previously reported compounds. Their structures were determined via interpreting spectroscopic data. Compounds **1** and **3**–**6** were found to possess radical scavenging activities and neuroprotective effects against oxidative stress in both neuronal cells. Hence, *Senna tora* sprouts and their constituents may be developed as natural neuroprotective agents via antioxidative effects.

1. Introduction

Reactive oxygen species (ROS) are oxygen-containing reactive molecules naturally produced in cellular metabolism. These molecules are constantly generated and eliminated in normal cellular physiology and play a critical role in the regulation of signal transduction pathways [1]. However, the balance between the generation and elimination of ROS is somehow disturbed due to endogenous and exogenous factors [1]. Glutamate is a critical excitatory neurotransmitter in several nervous systems, but excessive glutamate leads to the accumulation of intracellular ROS by blocking the cysteine uptake into neuronal cells through the cystine/glutamate antiporter, resulting in neuronal damages by oxidative stress [2,3]. These damages commonly lead to acute and chronic neuronal diseases [4]. Therefore, discovering antioxidants such as phenolic compounds represents promising strategies for these diseases.

Sprouts, commonly grown from any plant or vegetable seed, have long been used as an ingredient in oriental diets. Recently, their popularity has been steadily increasing in the world as consumers seek inexpensive, natural, and healthy foods [5,6]. Sprouts have been known to be a rich source of various nutrients including health-promoting phytochemicals with antioxidants properties. Several reports have shown that these phytochemicals are increased after germination, demonstrating that sprouts can provide several health benefits beyond basic nutrition [7–9].

Senna tora (L.) Roxb., an annual shrub belonging to the family Fabaceae, grows up to 30–90 cm tall with pinnate leaves and is widely cultivated in Asian countries [10]. Immature leaves are edible, and in particular, ripe seeds, Cassiae semen, have long been used to treat dizziness and headache, and to improve eye health as a roasted tea [11].

* Corresponding authors.
E-mail addresses: dsjang@khu.ac.kr (D.S. Jang), hkwon@kist.re.kr (H.C. Kwon).
[1] These authors contributed equally to this work.

https://doi.org/10.1016/j.bioorg.2021.105112
Received 26 February 2021; Received in revised form 16 June 2021; Accepted 18 June 2021
Available online 23 June 2021

Table 1
NMR data for compounds **1** and **2** in methanol-d_4.

Position	**1**		**2**	
	δ_C	δ_H, mult (*J* in Hz)	δ_C	δ_H, mult (*J* in Hz)
2	170.1		170.0	
3	105.8	6.12, s	110.7	6.36, s
4	184.1		184.5	
4a	102.5		109.8	
5	160.9		157.2	
5a	106.2			
6	154.7		106.6	6.90, s
6a			142.5	
7	111.9		100.7	6.84, d (2.0)
8	161.3		163.1	
9	97.0	6.92, s	102.2	6.79, d (2.0)
9a	139.8			
10	101.4	7.18, s	157.7	
10a	152.4		106.4	
10b			157.2	
11	19.4	2.41, s	20.5	2.59, s
1′	150.9		102.1	5.15, d (8.0)
2′	122.4		75.2	3.69, m
3′	132.4		78.5	3.53, t (8.8)
4′	120.6		71.6	3.41, t (8.8)
4′a	137.1			
5′	102.9	6.34, br s	77.1	3.68, m
6′	156.2		68.9	4.05, dd (11.2, 1.6)
				3.63, dd (11.2, 6.8)
7′	102.8	6.97, d (2.0)		
8′	156.1			
8′a	108.4			
9′	208.1			
10′	31.4	2.63, s		
11′	16.1	1.98, s		
1″	103.1	5.12, dd (8.0, 3.5)	111.1	4.95, d (2.4)
2″	73.5	3.58, t (8.5)	78.2	3.90, d (2.4)
3″	76.7	3.51, m	80.5	
4″	69.7	3.48, t (9.0)	75.1	3.99, d (9.6)
				3.74, d (9.6)
5″	77.4	3.55, dd (5.0, 2.0)	65.8	3.58, br s
6″	61.0	3.98, dd (12.0, 2.0)		
		3.78, dd (12.0, 5.0)		
OCH_3	54.8	3.75, s	56.1	3.93, s

Phytochemical investigations of this plant have revealed the presence of phenolic constituents, such as anthraquinones, naphthopyrone glycosides, and naphthalene glycosides, which have been found to have a broad range of biological activities, including antitumor, antigenotoxic, anti-inflammatory, and antihepatotoxic effects [10,12–15].

In screening to compare the abilities of *S. tora* seeds and sprouts to scavenge ROS, the extracts from sprouts showed improved activities in 2,2′-azino-bis(3-ethylbenzothiazoline-6-sulfonic acid) (ABTS) and 2,2-diphenyl-1-picrylhydrazyl (DPPH) assays. Also, the extracts from plant sprouts showed better neuroprotective activities against glutamate-induced oxidative stress in HT22 hippocampal neuronal (HT22) and R28 retina precursor (R28) cells. In general, antioxidative activity is considered as one of the key factors for neuronal cell protection. Hence, this study aimed to isolate as many components as possible observed as peaks in the HPLC chromatogram of the *S. tora* sprouts extract to identify the biologically active compounds and evaluate the possibility of the sprout as a functional food.

2. Experimental

2.1. General experimental procedures

Optical rotations were acquired on a Perkin-Elmer Model 343 polarimeter. UV spectra were measured on a Perkin-Elmer Lambda 35 UV/vis spectrophotometer. IR spectra were obtained using a Thermo Scientific Nicolet iS50 FT-IR spectrometer. ECD spectra were obtained via a Jasco J-1100 spectropolarimeter. NMR data were acquired on Varian 500 MHz, Bruker Avance III 400 MHz, and Bruker Avance III HD 800 MHz NMR spectrometers. HRESIMS data were obtained on Bruker MicrOTOF-Q II and AB Sciex TripleTOF 5600 mass spectrometers. Online HPLC-ABTS screening was performed on an Agilent 1200 HPLC system with a YMC Pack ODS-A column (5 μm, 150 × 4.6 mm). Preparative HPLC was performed using Gilson 321, YMC LC-Forte/R, and Jasco LC-2000Plus HPLC systems with Phenomenex Luna C18 (2) (10 μm, 250 × 21.2 mm), Phenomenex Luna C18(2) (10 μm, 250 × 10 mm), and Waters Delta-Pak C18 (15 μm, 300 × 30 mm) columns. Column chromatography was performed using Merck silica gel. TLC was carried out on a Merck pre-coated silica gel plate.

2.2. Plant materials

The seeds of *Senna tora*, cultivated in Goryeong, Republic of Korea, were purchased from a herbal market in Yeongcheon, Republic of Korea. The seeds were sterilized with 20 mg/mL of calcium hypochlorite for 15 min, rinsed thoroughly, and then soaked in distilled water for 4 h. Sterilized seeds were transferred to a tray and cultured in a growth chamber at 22 ± 3 °C, and distilled water was supplied every day. A fluorescent lamp, a 385 nm LED, a 465 nm LED, a 645 nm LED, and a 780 nm LED were used to investigate the effects of light conditions on producing compounds compared to dark conditions. After 7 d, the sprouts were collected and dried at 30 °C for 1 d. A voucher specimen (STS) was maintained at the KIST Gangneung Institute of Natural Products, Korea Institute of Science and Technology.

2.3. Extraction and isolation

The dried seeds (3.5 g) of *S. tora* were ground and extracted with ethanol (35.0 mL) for 7 d. The extract was evaporated to obtain a dark brown extract (117.3 mg). The dried sprouts (698.4 g) of *S. tora* cultivated in dark conditions were ground and extracted with ethanol (EtOH) (2 × 5.5 L) for 7 d. After evaporation, the obtained extract (66.7 g) was partitioned using deionized water (0.6 L) with ethyl acetate (EtOAc) (4 × 1.8 L) followed by *n*-buthanol (*n*-BuOH) (4 × 1.8 L). The EtOAc layer (23.5 g) was chromatographed on a silica gel column (*n*-hexane/chloroform/methanol, 1:1:0 to 0:1:1) to obtain twenty fractions (F_1–F_{20}). F_8 (1.4 g) was isolated by preparative HPLC (prep-HPLC) (acetonitrile/water, 3:2 to 1:0, flow rate 10.0 mL/min) to obtain 25 fractions ($F_{8.1}$–$F_{8.25}$). Among them, $F_{8.5}$ and $F_{8.8}$ were found to be isotoralactone (**3**, 7.5 mg, t_R = 36.8 min) and chrysophanol (**24**, 6.2 mg, t_R = 48.1 min), respectively. $F_{8.9}$ (21.6 mg) was isolated by prep-HPLC (acetonitrile/water, 3:2 to 9:1, flow rate 8.0 mL/min) to afford physcion (**25**, 0.8 mg, t_R = 21.9 min). $F_{8.11}$ (12.1 mg) was separated by prep-HPLC (acetonitrile/water, 3:2 to 1:0, flow rate 8.0 mL/min) to obtain chrysophanol-10,10′-bianthrone (**28**, 2.5 mg, t_R = 65.4 min). F_{12} (2.1 g) was isolated by prep-HPLC (acetonitrile/water, 2:3 to 1:0, flow rate 10.0 mL/min) to obtain 27 fractions ($F_{12.1}$–$F_{12.27}$). $F_{12.11}$ (14.7 mg) was separated by prep-HPLC (acetonitrile/water, 19:31, flow rate 8.0 mL/min) to afford aurantio-obtusin (**26**, 0.8 mg, t_R = 27.3 min) and chryso-obtusin (**27**, 0.9 mg, t_R = 45.6 min). $F_{12.17}$ (32.3 mg) was separated by prep-HPLC (acetonitrile/water, 13:7 to 1:0, flow rate 8.0 mL/min) to afford toralactone (**4**, 1.2 mg, t_R = 24.2 min) and emodin-physcion bianthrone (**29**, 0.5 mg, t_R = 62.8 min). F_{13} (135.5 mg) was separated by prep-HPLC (acetonitrile/water, 1:9 to 1:0, flow rate 8.0 mL/min) to obtain torosachrysone (**5**, 0.6 mg, t_R = 71.3 min) and rubrofusarin (**6**, 2.6 mg, t_R = 120.7 min). F_{15} (893.7 mg) was separated by prep-HPLC (acetonitrile/water, 3:7, flow rate 8.0 mL/min) to afford cassialactone (**7**, 0.7 mg, t_R = 192.4 min). F_{16} (1.5 g) was fractionated on a silica gel column (methylene chloride/methanol, 20:1 to 1:1) to obtain 14 fractions ($F_{16.1}$–$F_{16.14}$). $F_{16.3}$ (46.2 mg) was separated by prep-HPLC (acetonitrile/water, 1:4 to 1:0, flow rate 8.0 mL/min) to afford 7-*O*-methylkaempferol (**19**, 1.8 mg, t_R = 30.1 min), quercetin (**18**, 1.9 mg, t_R = 34.7 min), and 7-*O*-methylquercetin (**20**, 1.0 mg, t_R = 38.9 min). $F_{16.4}$ (78.3 mg) was separated by prep-HPLC (acetonitrile/water, 1:4 to 1:0, flow rate 6.5

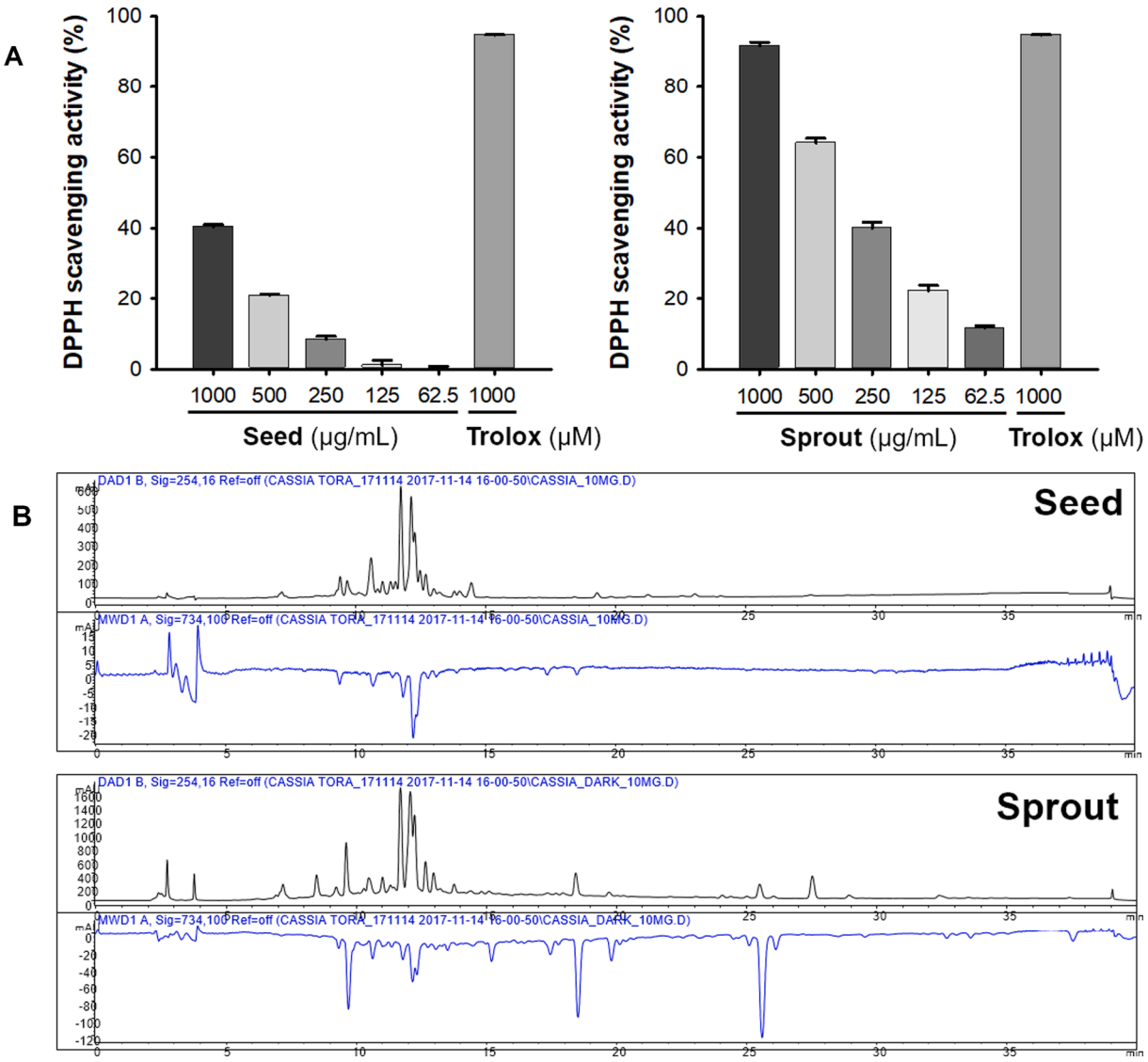

Fig. 1. Radical scavenging activities of the extracts from *S. tora* seed and sprout assessed by DPPH (A) and on-line HPLC-ABTS (B) assays.

mL/min) to afford 1-[(3-methoxyl-8-hydroxyl-1-*O*-*β*-glucopyranosylnaphthalen)-6-yl]propan-2-one (**15**, 2.5 mg, t_R = 22.9 min), 6-hydroxymusizin-8-*O*-*β*-glucopyranoside (**16**, 2.1 mg, t_R = 26.2 min), and torachrysone-8-*O*-*β*-glucopyranoside (**8**, 0.5 mg, t_R = 68.1 min). $F_{16.6}$ (98.7 mg) was separated by prep-HPLC (acetonitrile/water, 17:83 to 1:0, flow rate 6.5 mL/min) to obtain cassialactone-9-*O*-*β*-glucopyranoside (**9**, 2.0 mg, t_R = 77.2 min). $F_{16.7}$ (422.7 mg) was separated by prep-HPLC (acetonitrile/water, 1:4 to 1:0, flow rate 6.5 mL/min) to obtain cassiaside A (**10**, 4.1 mg, t_R = 92.3 min). F_{17} (2.4 g) was separated by prep-HPLC (acetonitrile/water, 1:9 to 1:0, flow rate 6.5 mL/min) to give cassiaside B (**11**, 1.7 mg, t_R = 197.3 min). F_{18} (3.7 g) was fractionated on a silica gel column (methylene chloride/methanol, 20:1 to 1:1) to afford 24 fractions ($F_{18.1}$–$F_{18.24}$). $F_{18.17}$ (124.8 mg), $F_{18.18}$ (226.9 mg), $F_{18.20}$ (112.0 mg), and $F_{18.21}$ (110.6 mg) were combined and isolated by prep-HPLC (acetonitrile/water, 1:9 to 1:0, flow rate 6.5 mL/min) to afford nepalenside A (**17**, 24.8 mg, t_R = 42.1 min), quercetin-3-*O*-neohesperidoside (**22**, 4.1 mg, t_R = 85 min), kaempferol-3-*O*-neohesperidoside (**23**, 6.4 mg, t_R = 99.3 min), quercetin-3-*O*-*β*-glucopyranoside (**21**, 5.5 mg, t_R = 104.6 min), demethylflavasperone-10-*O*-*β*-D-glucopyranosyl-6-*O*-*β*-D-apiofuranoside (**2**, 1.6 mg, t_R = 140.2 min), demethylflavasperone-10-*O*-*β*-glucopyranoside (**13**, 2.3 mg, t_R = 142.3 min), rubrofusarin-6-*O*-*β*-gentiobioside (**14**, 0.6 mg, t_R = 155.7 min), cassiaside C (**12**, 9.3 mg, t_R = 177.6 min), and 7-hydroxymusizinyl-rubrofusarin-8′-*O*-*β*-D-glucopyranoside (**1**, 5.6 mg, t_R = 221.2 min).

2.3.1. 7-Hydroxymusizinyl-rubrofusarin-8′-O-β-D-glucopyranoside (1)

Yellowish amorphous solid; $[\alpha]^{20}_D$ –20.0 (*c* 0.05, methanol); UV (0.15 mM, methanol) λ_{max} (log ε) 225 (4.32), 282 (4.23) nm; IR ν_{max} (ATR) 3387, 2940, 1682, 1650, 1622, 1471, 1430, 1361, 1096 cm^{-1}; ECD (*c* 1.0 mM, acetonitrile) $\Delta\varepsilon$ + 8.4 (235), –0.5 (261), +4.2 (293), –0.8 (329); ^1H and ^{13}C NMR data (methanol-d_4), see Table 1; ESIMS (negative) *m/z* 663 $[M - H]^-$; ESIMS (positive) *m/z* 665 $[M + H]^+$; HRESIMS (positive) *m/z* 665.1860 $[M + H]^+$ (calcd for $C_{34}H_{33}O_{14}$, 665.1865).

2.3.2. Demethylflavasperone-10-O-β-D-glucopyranosyl-6-O-β-D-apiofuranoside (2)

White amorphous solid; $[\alpha]^{20}_D$ –54.0 (*c* 0.05, methanol); UV (0.18 mM, methanol) λ_{max} (log ε) 240 (4.09), 279 (3.95), 366 (3.15) nm; IR ν_{max} (ATR) 3405, 2922, 1677, 1622, 1439, 1206, 1134 cm^{-1}; ^1H and ^{13}C NMR data (methanol-d_4), see Table 1; ESIMS (negative) *m/z* 565 $[M - H]^-$; ESIMS (positive) *m/z* 567 $[M + H]^+$; HRESIMS (positive) *m/z* 567.1703 $[M + H]^+$ (calcd for $C_{26}H_{31}O_{14}$, 567.1708).

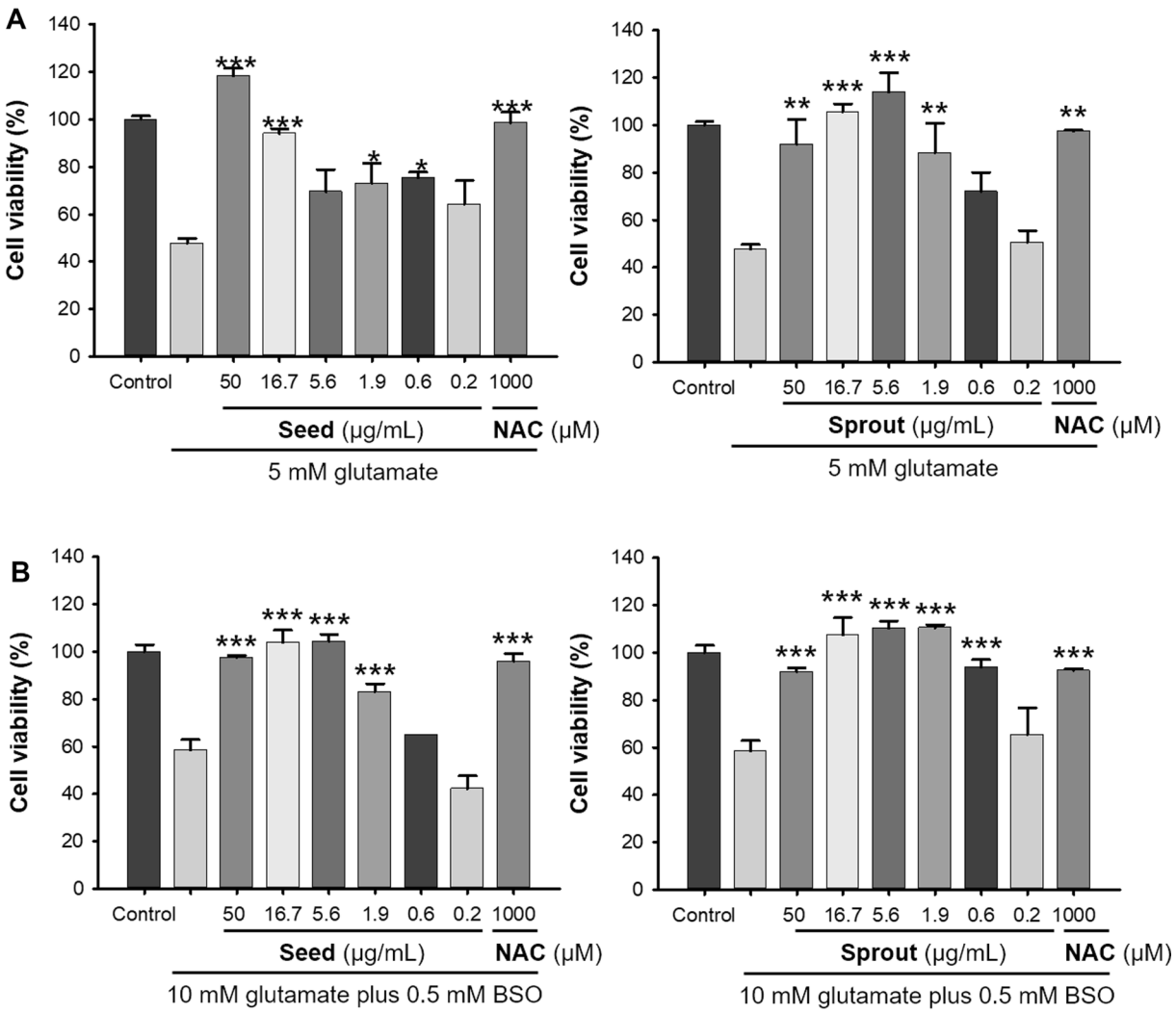

Fig. 2. Neuroprotective effects of the extracts from *S. tora* seed and sprout against glutamate-induced oxidative stress in HT22 (A) and R28 (B) cells.

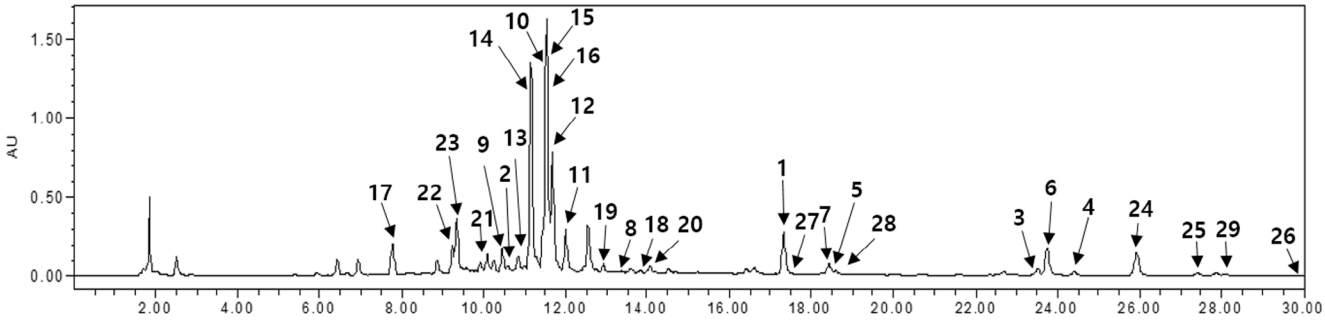

Fig. 3. HPLC chromatogram of the extracts from *S. tora* sprout.

2.4. Acid hydrolysis and absolute configuration determination of sugar moieties

Compounds **1** and **2** (each 0.5 mg) were separately treated with 1 M of hydrochloric acid (500 μL) at 104 °C for 3 h, followed by a partition with ethyl acetate (4 × 2.0 mL) to obtain each aglycone. The aqueous layers containing sugars were evaporated, dissolved in pyridine (100 μL), and treated with 0.5 mg of L-cysteine methyl ester hydrochloride at 60 °C for 1.5 h, followed by a reaction with *O*-tolylisothiocyanate (25 μL) at 60 °C for 1.5 h and direct analysis via reverse-phased HPLC in linear gradients. The thiocarbamoyl-thiazolidine carboxylate derivatives of the monosaccharides obtained from **1** and **2** were determined by comparing the retention times with those of the authentic samples (t_R: D-glucose 14.6 min and D-apiose 19.3 min).

2.5. Computational methods

Electronic circular dichroism (ECD) calculations were performed according to a previously reported method [16]. Briefly, 3D modeling was carried out using the Chem3D program followed by conformational

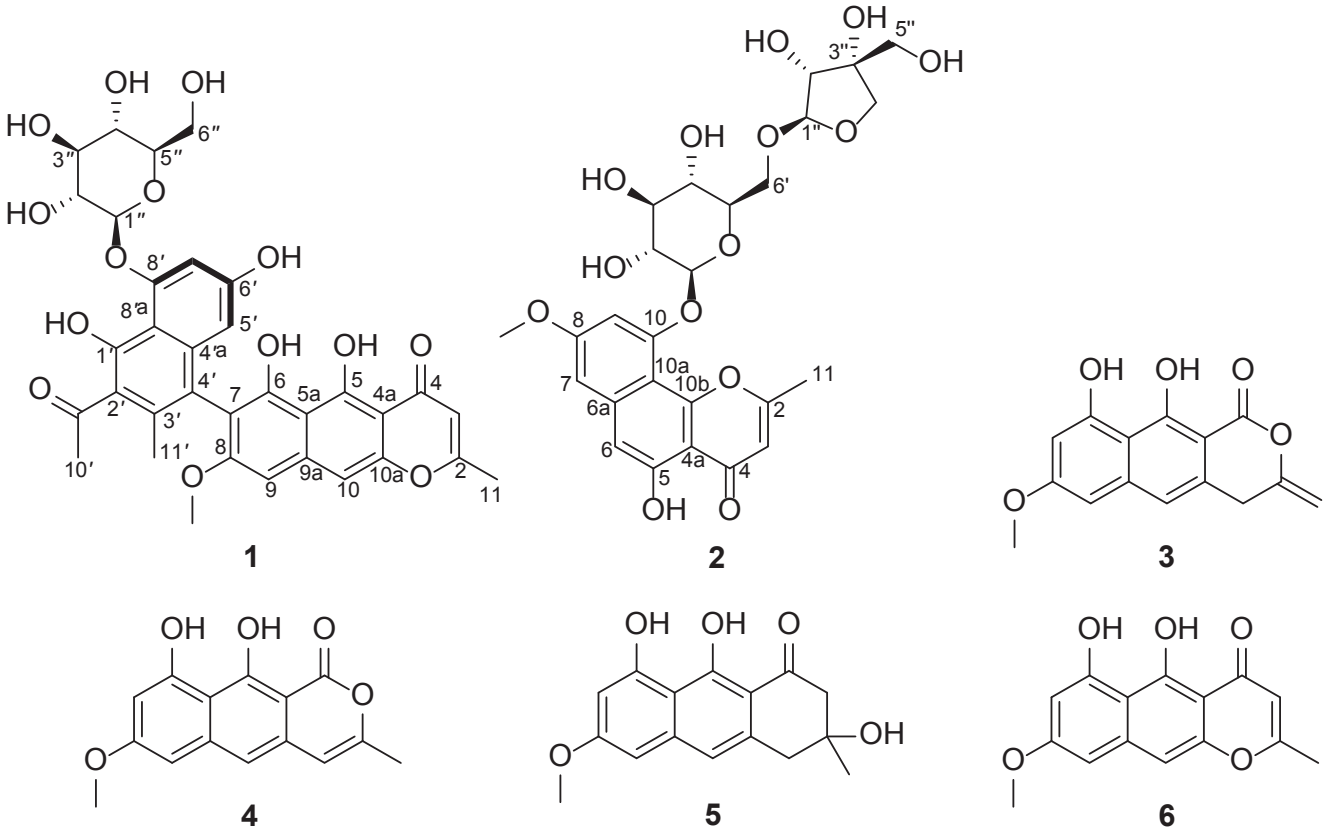

Fig. 4. Structures of the isolated compounds **1**–**6**.

searches via the Merck Molecular Force Field in the Spartan′14 software, optimization using a density functional theory (DFT) calculation with B3LYP/6–31+G(d.p) in the Gaussian 09 package, and a time-dependent DFT calculation with CAM-B3LYP/SVP in acetonitrile. The computed ECD spectra were visualized using SpecDis 1.64 software followed by applying Boltzmann distribution with UV correction [17].

2.6. Antioxidative activity

The scavenging effects of samples for DPPH radicals were assessed based on a previous report [18]. Briefly, DPPH (0.1 mM) in methanol (100 μL) was mixed with various concentrations of samples (100 μL) for 1 h in the dark. The absorbance was recorded at 517 nm.

An online HPLC-ABTS assay was performed as referenced in several reports, with modifications [19]. ABTS reagent was prepared as a mixture containing ABTS (0.07 mM) with potassium persulfate (0.12 mM) and stored in darkness at 4 °C for 12 h to stabilize radicals. All samples were analyzed via HPLC (acetonitrile/water containing 0.02% TFA, 1:9 to 1:0, flow rate 0.7 mL/min). The eluate was then sent to a *T*-junction and reacted with ABTS reagent in a reaction coil at 40 °C. The chromatogram was visualized at 254 nm (positive peak), as well as at 734 nm (negative peak), to record the decrease in ABTS radicals.

2.7. Neuroprotective activity against glutamate-induced oxidative stress in HT22 cells

HT22 mouse hippocampal neuronal cells were purchased from the Korean Cell Line Bank (Seoul, South Korea) and were cultivated in low-glucose Dulbecco's modified eagle's medium (DMEM) with 10% fetal bovine serum (FBS) and penicillin/streptomycin (100 U/mL) at 37 °C under 5% CO_2 with humidified air. Cell viability was determined by a 3-(4,5-dimethylthiazol-2-yl)-2,5-diphenyltetrazolium bromide (MTT) assay. HT22 cells were plated in 96-well plates at a density of 3×10^3 cells/well and incubated for 24 h. Subsequently, the cells were treated with various concentrations of samples over 2 h, followed by the addition of glutamate (5 mM) and incubation for 22 h. The measurement of cell viability was performed via an EZ-Cytox Assay Kit (Daeil lab service) for 2 h. The absorbance was recorded at 450 nm using a Molecular Devices FilterMax F5 microplate reader.

2.8. Neuroprotective activity against glutamate-induced oxidative stress in R28 cells

R28 retinal cells were purchased from Kerafast (Kerafast, Inc., Boston, MA, USA) and were cultured under the same conditions as HT22 cells. Cell viability was determined by performing an MTT assay. R28 cells were seeded in 96-well plates at a density of 1×10^4 cells/well and incubated for 24 h. Subsequently, the cells were treated with various concentrations of samples over 2 h, followed by the addition of glutamate (10 mM) plus BSO (0.5 mM) (glutamate/BSO) and incubation for 22 h. The measurement of cell viability was performed via an EZ-Cytox Assay Kit (Daeil lab service) for 2 h. The absorbance was recorded at 450 nm.

2.9. Inhibitory activity against glutamate-induced intracellular ROS generation

HT22 cells were added in 96-well black/clear bottom plates at 3×10^3 cells/well and incubated at 37 °C under 5% CO_2 for 24 h. The indicated concentrations of compounds **1**, **3**, **4**, **5**, and **6** were added to 96-well plates, and 0.5% dimethyl sulfoxide (DMSO) was used for control. After 2 h, cells were treated with glutamate (5 mM) and incubated for 8 h. After incubation, media were replaced with serum-free ones. Cells were treated with 2′,7′-dichlorodihydrofluorescein diacetate (5 μM) for staining. After 30 min, serum-free media (50 μL, twice) were added for washing, and cells were analyzed by an Operetta image

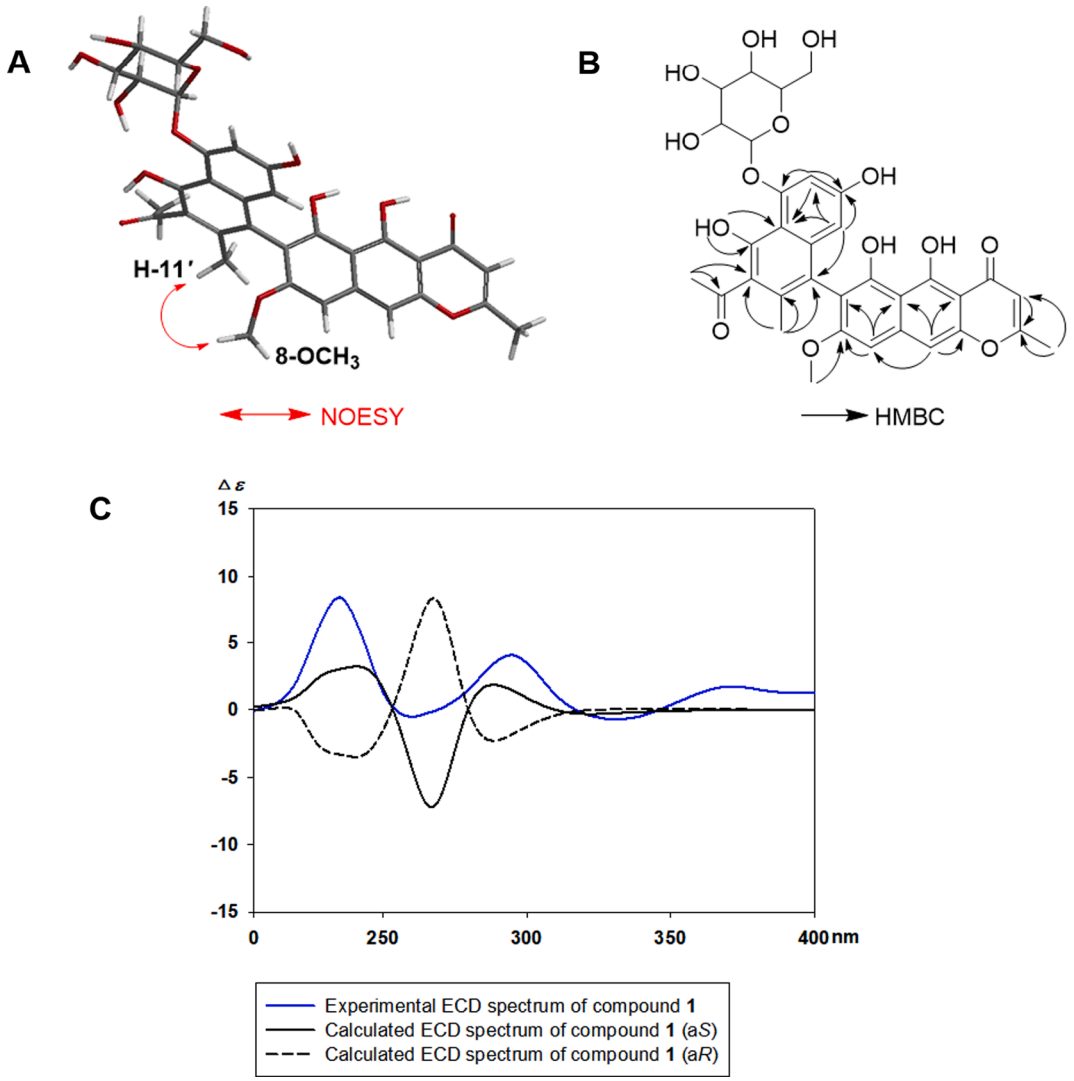

Fig. 5. NOESY (A) and HMBC (B) correlations for compound **1** and measured and calculated ECD spectra of compound **1** (C).

analysis system.

R28 cells were added in 96-well plates at 1×10^4 cells/well and incubated at 37 °C under 5% CO_2 for 24 h. Cells were treated with indicated concentrations of five compounds, followed by the treatment of glutamate/BSO after 2 h. Incubation and image analysis of R28 cells were carried out under the same conditions as in the case of HT22 cells.

2.10. Inhibitory activity against glutamate-induced Ca^{2+} influx

HT22 cells were added in 96-well plates at 3×10^3 cells/well and incubated at 37 °C under 5% CO_2 for 24 h. Cells were treated with indicated concentrations of compounds **1**, **3**, **4**, **5**, and **6**, and 0.5% DMSO was used for control. After 2 h, cells were treated with glutamate (5 mM) and incubated for 8 h, followed by the replacement of media with HBSS and the addition of Flu-3 (2 μM) for staining. After 15 min, HBSS (50 μL, twice) was added for washing, and cells were analyzed by an Operetta image analysis system.

R28 cells were added in 96-well plates at 1×10^4 cells/well and incubated at 37 °C under 5% CO_2 for 24 h. Cells were treated with five compounds, followed by the treatment of glutamate/BSO after 2 h. Incubation and image analysis of R28 cells were performed under the same conditions as in the case of HT22 cells.

2.11. Statistical analysis

Statistical differences were evaluated using one-way ANOVA followed by Tukey-HSD post hoc test for multiple group comparisons.

3. Results and discussion

3.1. Antioxidative and neuroprotective activities of S. tora seed and sprout

The antioxidative activities of the extracts from *S. tora* seeds and sprouts were evaluated as preliminary screening using DPPH and online HPLC-ABTS assays. The extract from the sprouts was found to be approximately 2 times more active than that from the seeds in the DPPH assay (Fig. 1A), and the online HPLC-ABTS assay showed similar results (Fig. 1B). From the comparison between chromatograms of the extracts from the sprouts and seeds, it was inferred that this was due to the newly produced or increased amounts of phenolic compounds that were eluted after 15 min (Fig. 1B). To investigate whether these compounds were changed or stably produced during germination and growth processes, sprouts were cultivated by controlling light conditions (fluorescent lamp, 385 nm LED, 465 nm LED, 645 nm LED, and 780 nm LED) for seven days. No distinct effects of these light conditions on producing target compounds were observed. Hence, the dark condition was

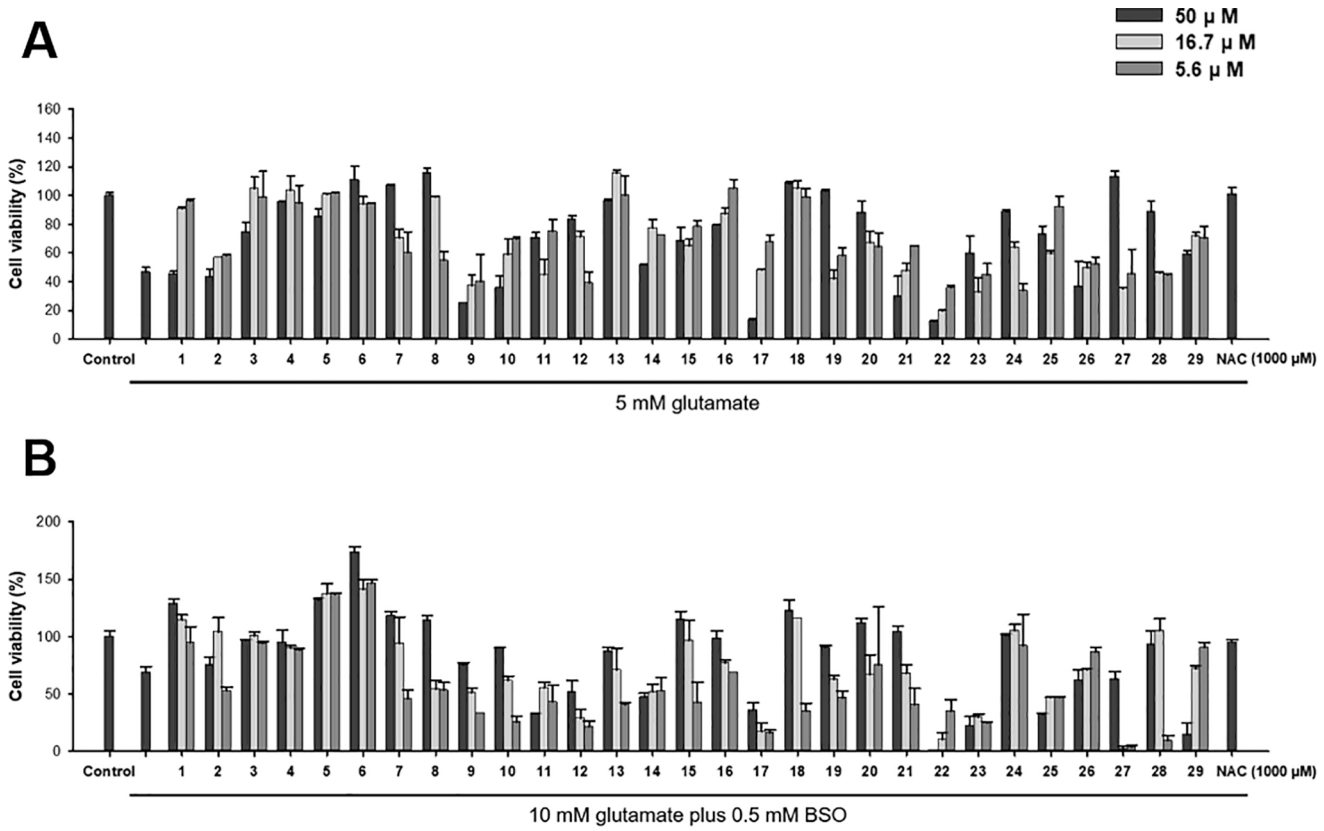

Fig. 6. Neuroprotective effects of all isolated compounds against glutamate-induced oxidative stress in HT22 (A) and R28 (B) cells.

selected for large cultivation since these compounds were the most produced (Fig. S1). Then an evaluation of the neuroprotective effects was carried out, which was closely related to the antioxidative activity. The neuroprotective effects of the extracts from *S. tora* seeds and sprouts, against glutamate-induced oxidative stress in HT22 cells and glutamate/BSO-induced oxidative stress in R28 cells, were evaluated. The extract from the sprouts was found to be more active than that from the seeds in both cells (Fig. 2).

3.2. Phytochemical investigation

To explore these phenolic constituents, various chromatographic and spectroscopic methods for separation, isolation, and structural elucidation were applied. Two new naphthopyrone glycosides (**1** and **2**) were obtained from the EtOAc layer of EtOH extract of *S. tora* sprouts, along with 27 known compounds, namely isotoralactone (**3**) [20], toralactone (**4**) [21], torosachrysone (**5**) [20], rubrofusarin (**6**) [22], cassialactone (**7**) [23], torachrysone-8-*O*-*β*-glucopyranoside (**8**) [24], cassialactone-9-*O*-*β*-glucopyranoside (**9**) [25], cassiasides A–C (**10**–**12**) [21,26], demethylflavasperone-10-*O*-*β*-glucopyranoside (**13**) [27], rubrofusarin-6-*O*-*β*-gentiobioside (**14**) [21], 1-[(3-methoxyl-8-hydroxyl-1-*O*-*β*-glucopyranosylnaphthalen)-6-yl]propan-2-one (**15**) [28], 6-hydroxymusizin-8-*O*-*β*-glucopyranoside (**16**) [24], nepalenside A (**17**) [29], quercetin (**18**) [30], 7-*O*-methylkaempferol (**19**) [31], 7-*O*-methylquercetin (**20**) [32], quercetin-3-*O*-*β*-glucopyranoside (**21**) [30], quercetin-3-*O*-neohesperidoside (**22**) [33], kaempferol-3-*O*-neohesperidoside (**23**) [34], chrysophanol (**24**) [35], physcion (**25**) [35], aurantio-obtusin (**26**) [36], chryso-obtusin (**27**) [36], chrysophanol-10,10′-bianthrone (**28**) [22], and emodin-physcion bianthrone (**29**) [37] by comparing the NMR and MS data with data reported in the literature (Fig. 3 and S17, Supporting Information) (see Fig. 4).

Compound **1** was isolated as a yellowish and amorphous solid having the molecular formula $C_{34}H_{32}O_{14}$, consistent with 19 degrees of unsaturation, based on the peak at *m/z* 665.1860 $[M + H]^+$ in the HRESIMS. In particular, the fragments in the positive mode at *m/z* 503, 489, 461, and 272 suggested the presence of glucose and additional naphthalene or naphthopyrone derivatives, including compound **6**. The IR spectrum suggested that hydroxy groups (3387 cm^{-1}), carbonyl groups (1622 and 1650 cm^{-1}), and aromatic rings (2940 and 1583 cm^{-1}) were present. The ^1H NMR data (Table 1) suggested the characteristic pattern of a naphthopyrone skeleton, which exhibited five methine signals (δ_H 7.18, 6.97, 6.92, 6.34, and 6.12) in the aromatic and olefinic regions, three methyl signals (δ_H 2.63, 2.41, and 1.98), and a methoxy signal (δ_H 3.75). Furthermore, the signals for a typical *β*-glucose moiety were observed (δ_H 5.12, 3.98, 3.78, 3.58, 3.55, 3.51, and 3.48). The ^{13}C NMR data (Table 1) revealed the presence of three methyl carbons, one methoxy carbon, one methylene carbon, 10 methine carbons, including one olefinic, four aromatic, and five oxygenated carbons, two carbonyl carbons, eight oxygenated tertiary carbons, and nine quaternary carbons. The complete assignment of these NMR data demonstrated the structure of **1** as consisting of isolated **6** and **16** units, and the presence of two quaternary carbon signals at C-7 and C-4′ (δ_C 111.9 and 120.6) suggested that these components were unsymmetrically dimerized through a 7–4′ linkage. This dimerization was further evidenced by the NOESY correlation of H-11′ and 8-OCH_3 (Fig. 5A). The position of the *β*-glucose moiety was deduced to be attached at C-8′ according to a HMBC cross-peak of H-1″ and C-8′ (δ_C 156.1), and the comprehensive interpretation of the 2D NMR data, including HMBC correlation (Fig. 5B), confirmed the planar structure of **1**. The *β*-glucose unit was determined to have a D-form by comparison with an authentic standard sample via the HPLC method, conducted as referenced in a previous report (Fig. S15, Supplementary material) [38]. The axial configuration between the two components was determined using the exciton chirality method using ECD. The ECD spectra of **1** showed a positive Cotton effect (CE) at 293 nm ($\Delta\varepsilon$ + 4.2) and a negative CE at 261 nm ($\Delta\varepsilon$ –0.5). This positive exciton chirality was due to

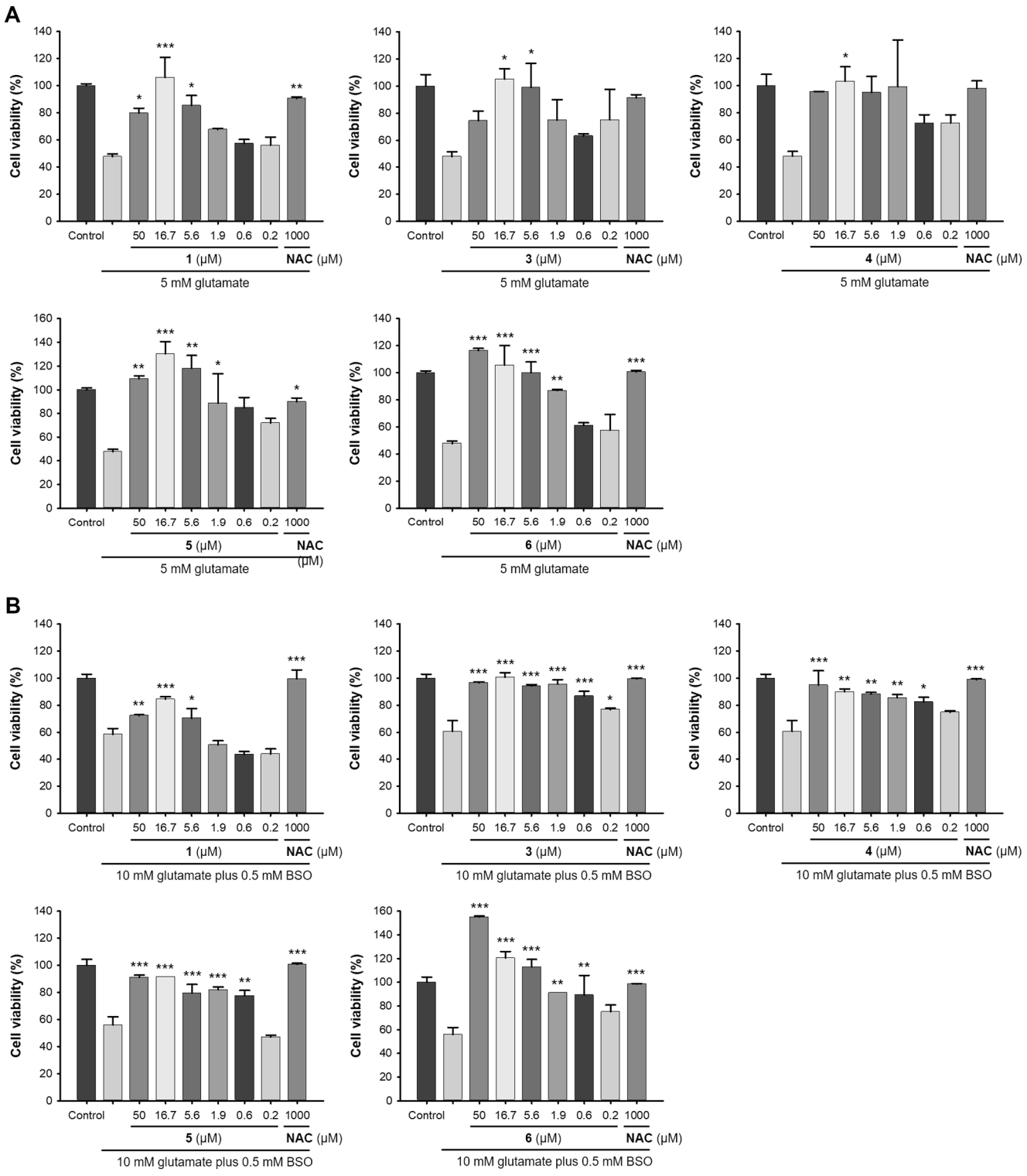

Fig. 7. Neuroprotective effects of compounds **1** and **3**–**6** against glutamate-induced oxidative stress in HT22 cell (*$P < 0.05$, **$P < 0.01$ and ***$P < 0.001$) (A) and against glutamate-induced oxidative stress in R28 cell (*$P < 0.05$, **$P < 0.01$ and ***$P < 0.001$) (B).

couplings between ^1B_b transitions of the naphthopyrone chromophores and demonstrated that the two axes are configured in a clockwise screw, suggesting an (a*S*)-configuration. This result was supported by the ECD data of previously reported naphthopyrones [39]. Furthermore, the ECD calculation method using two possible models (a*S* and a*R*) was applied to clarify our result. The calculated ECD data of the a*S* model was closely fitted well with the experimental ECD data (Fig. 5C). Consequently, compound **1** was assigned as 7-hydroxymusizinyl-rubrofusarin-8′-*O*-*β*-D-glucopyranoside.

Compound **2** was found to have the molecular formula $C_{26}H_{30}O_{14}$ via HRESIMS. The complete assignment of the 1D NMR data (Table 1) demonstrated its structure to be superimposable on that of **13**, except for the presence of an additional *β*-apiose moiety. The position of the *β*-apiose moiety was deduced to be connected at C-6′ of a *β*-glucose moiety, which was indirectly suggested by the downfield shift of the ^{13}C NMR signal at C-6′ (δ_C 68.9). Both sugar units were demonstrated to

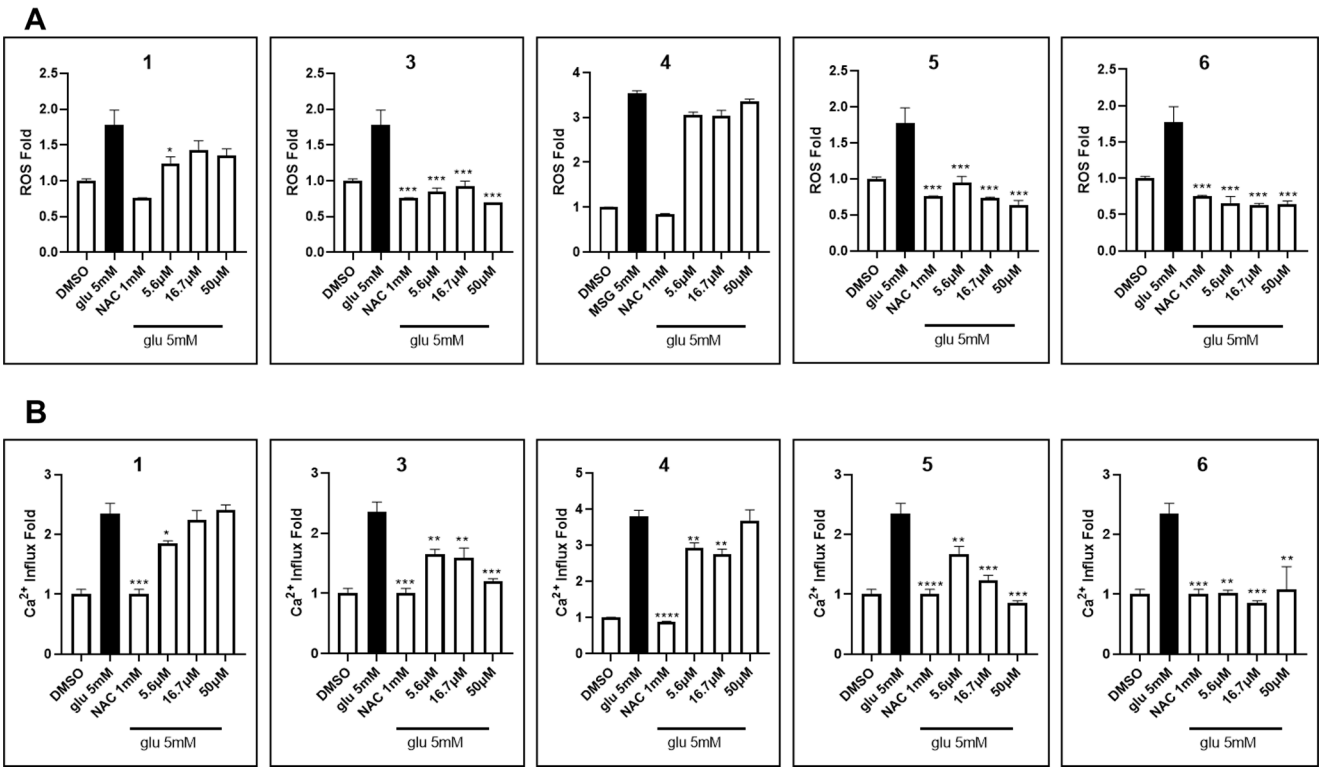

Fig. 8. Inhibitory effects of compounds **1** and **3**–**6** against glutamate-induced intracellular ROS generation (A) and Ca^{2+} influx (B) in HT22 cell (*$P < 0.05$, **$P < 0.01$, ***$P < 0.001$, and ****$P < 0.0001$).

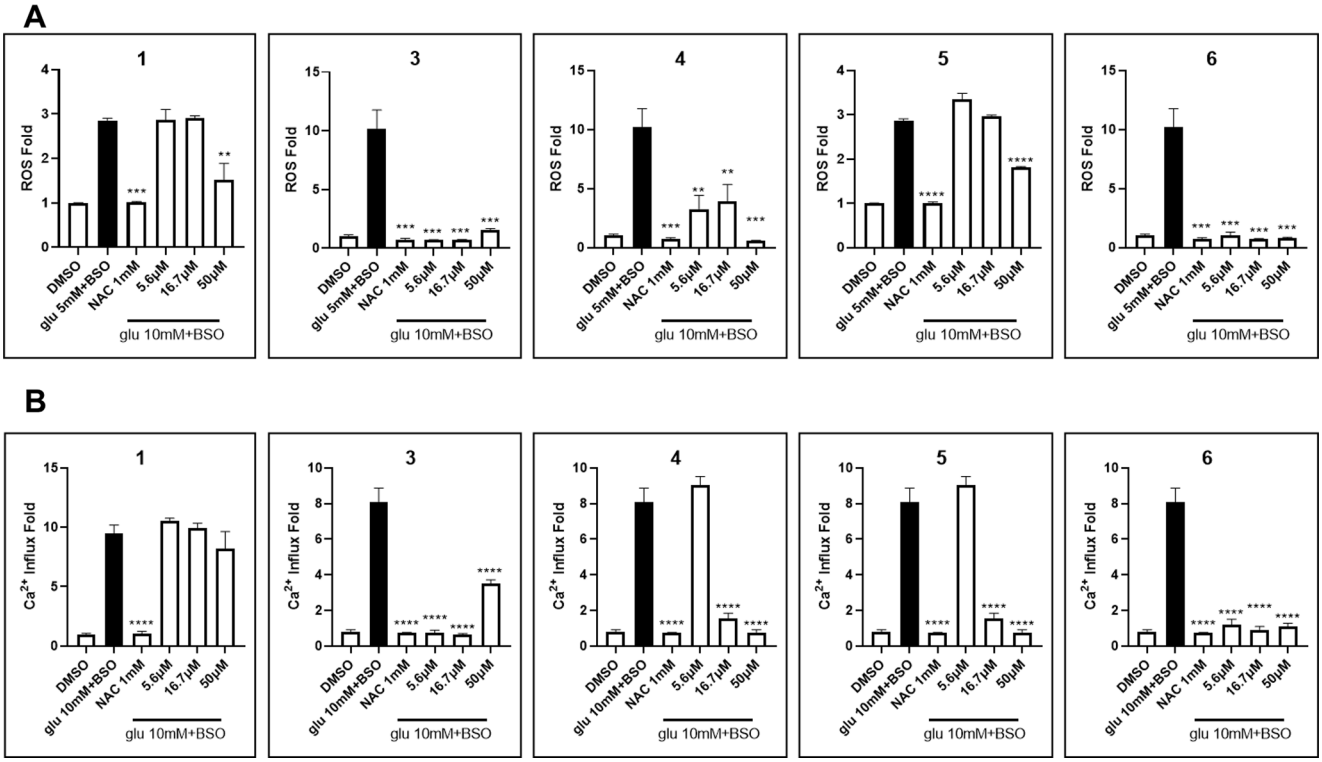

Fig. 9. Inhibitory effects of compounds **1** and **3**–**6** against glutamate-induced intracellular ROS generation (A) and Ca^{2+} influx (B) in R28 cell (*$P < 0.05$, **$P < 0.01$, ***$P < 0.001$, and ****$P < 0.0001$).

possess a D-form according to the same HPLC method (Fig. S15, Supplementary material). Consequently, compound **2** was assigned as demethylflavasperone-10-*O*-*β*-D-glucopyranosyl-6′-*O*-*β*-D-apiofuranoside.

3.3. Antioxidative and neuroprotective activities of the isolated compounds

The antioxidative activities of all obtained compounds were rapidly evaluated using an online HPLC-ABTS assay with UV (254 nm, positive signal) and $ABTS^{+}$ quenching (734 nm, negative signal) chromatograms. Compounds **1**, **3**–**8**, **10**, **12**, **14**–**16**, and **18**–**22** were found to be active due to showing relatively strong signals, whereas the others exhibited weak or even no activities (Fig. S16, Supplementary material). Besides, all obtained compounds were assessed for their neuroprotective effects against glutamate-induced oxidative stress in HT22 cells and glutamate/BSO-induced oxidative stress in R28 cells, with *N*-acetyl-L-cysteine (NAC), used as a positive control. HT22 cells were treated with glutamate (5 mM) in the absence or presence of various concentrations of the compounds. Although cell viability was decreased to 45.7% after exposure to glutamate, compounds **1**, **3**–**6**, **13**, **16**, **18**, and **25** increased the viability to over 92.1% at the lowest concentration (5.6 μM) of the screening system, while NAC (1 mM) restored the viability to 101.0% (Fig. 6A). Also, R28 cells were treated with glutamate (10 mM)/BSO (0.5 mM) in the absence or presence of the compounds. Despite the reduction of the viability to 68.9%, due to excitotoxicity induced by glutamate/BSO, compounds **1**, **3**–**6**, and **24** increased cell viability to over 88.3% at 5.6 μM, whereas 1 mM of NAC restored the viability to 94.8% (Fig. 6B). Taken together, compounds **1** and **3**–**6** were found to be active in both cells (Table S1, Supplementary material) and were further analyzed for their neuroprotective potentials using a six-point serial concentration. An amount of 16.7 μM of compounds **1** and **3**–**5**, as well as 50.0 μM of **6**, exhibited more than a 105.1% neuroprotective effect in HT22 cells (Fig. 7A). Also, 16.7 μM of compounds **1**, **3**, and **5**, as well as 50.0 μM of **4** and **6**, showed a greater than 84.5% neuroprotective effect in R28 cells, based on their restoration of cell viability (Fig. 7B).

The above results demonstrate that compounds **1** and **3**–**6**, derived from sprouts with newly produced or an increased amount of naphthopyrones, were commonly active in the three experiments, and can protect neuronal HT22 and R28 cells via their antioxidative activities. Although the exact structure–activity relationship could not be demonstrated, in general, it was presumed that the activities of the isolated naphthopyrones could be increased by decreasing the number of sugar units, according to a comparison of the activities between compounds **2** and **13**, compounds **4** and **12**, compounds **6**, **11**, and **14**, and compounds **7** and **9**.

3.4. Inhibitory activities of the isolated compounds against glutamate-induced intracellular ROS generation and Ca^{2+} influx

It has been reported that glutamate induces the increase of cellular ROS and Ca^{2+} ions, which are involved in MAPK activation or cell death. Hence, the inhibitory activities of five compounds were evaluated on the glutamate-induced intracellular ROS formation in both HT22 and R28 cells. 2′,7′-Dichlorodihydrofluorescein diacetate was used as a ROS sensor since this molecule can penetrate the cell membrane and emit high fluorescence by reacting with superoxide, hydroxyl radicals, peroxide, etc [40]. The treatment of **3**, **5,** and **6** inhibited the production of cellular ROS in HT22 cells, whereas compounds **1** and **4** showed weak or no inhibitory activities (Fig. 8A). It was confirmed whether these compounds could affect glutamate-induced Ca^{2+} influx using a Fluo-3 fluorescence sensor. As with the above results, compounds **3**, **5**, and **6** showed potent effects on the prevention of Ca^{2+} influx, while the other compounds were not active (Fig. 8B). These results indicated that cell viability results of compounds **3**, **5**, and **6** in HT22 cells correlated with the inhibitory effects of ROS generation and Ca^{2+} influx.

The inhibitory effects of compounds were evaluated against glutamate-mediated intracellular ROS generation and Ca^{2+} influx in R28 cells. Compounds **3**, **4**, and **6** showed potent inhibitory effects against glutamate-induced ROS generation in R28 cells, while 50 μM of compounds **1** and **5** showed weak activities (Fig. 9A). Also, the treatment of compounds **3** and **6** showed potent inhibitory effects on Ca^{2+} influx. Even though 50 μM and 16.7 μM of compounds **4** and **5** exhibited potent inhibitory effects to glutamate-mediated Ca^{2+} influx, 5.6 μM of these compounds showed no activities (Fig. 9B). As a result, cell viability results of compounds **3**, **4**, **5**, and **6** in R28 cells correlated with ROS generation's inhibitory effects and Ca^{2+} influx.

4. Conclusion

Our initial findings demonstrated that the extracts of *S. tora* sprouts cultivated in the dark condition possess improved biological activities than those of seeds. These results were due to the creation of new constituents or the increased amount of existing phenolic compounds. Hence, we identified most constituents in the HPLC chromatogram and found the most potent neuroprotective antioxidants of *S. tora* (**1** and **3**–**6**). In particular, only a little has been reported on the dimerized form of naphthopyrone and naphthalene derivatives. This is the first report that dimerized compounds can have activities and be produced in *S. tora*. Although we found that some active compounds could prevent intracellular ROS generation and Ca^{2+} influx, further and more extensive studies, including mechanistic research, might be needed to develop *S. tora* sprouts and their constituents as valuable neuroprotective natural products.

Declaration of Competing Interest

The authors declare that they have no known competing financial interests or personal relationships that could have appeared to influence the work reported in this paper.

Acknowledgements

The research was financially supported by the Korea Institute of Science & Technology Program (2E31300) and the KHU-KIST Converging Science and Technology - Joint Research Program.

Appendix A. Supplementary material

Supplementary data to this article can be found online at https://doi.org/10.1016/j.bioorg.2021.105112.

References

[1] D.S. Simpson, P.L. Oliver, ROS generation in microglia: understanding oxidative stress and inflammation in neurodegenerative disease, Antioxidants 9 (8) (2020) 743.
[2] P. Maher, K. van Leyen, P.N. Dey, B. Honrath, A. Dolga, A. Methner, The role of Ca^{2+} in cell death caused by oxidative glutamate toxicity and ferroptosis, Cell Calcium 70 (2018) 47–55.
[3] E. Suárez-Pozos, Z. Martínez-Lozada, O.G. Méndez-Flores, A.M. Guillem, L. C. Hernández-Kelly, F. Castelán, T.N. Olivares-Bañuelos, D. Chi-Castañeda, M. Najimi, A. Ortega, Characterization of the cystine/glutamate antiporter in cultured Bergmann glia cells, Neurochem. Int. 108 (2017) 52–59.
[4] X. Zhang, D. Wang, B. Zhang, J. Zhu, Z. Zhou, L. Cui, Regulation of microglia by glutamate and its signal pathway in neurodegenerative diseases, Drug Discovery Today 25 (6) (2020) 1074–1085.
[5] Y. Yang, F. Meier, J. Ann Lo, W. Yuan, V. Lee Pei Sze, H.J. Chung, H.G. Yuk, Overview of recent events in the microbiological safety of sprouts and new intervention technologies, Compr. Rev. Food Sci. Food Saf. 12 (3) (2013) 265–280.
[6] S. Fischer, R. Wilckens, J. Jara, M. Aranda, W. Valdivia, L. Bustamante, F. Graf, I. Obal, Protein and antioxidant composition of quinoa (*Chenopodium quinoa* Willd.) sprout from seeds submitted to water stress, salinity and light conditions, Ind. Crops Prod. 107 (2017) 558–564.
[7] S.-L. Kim, S.-K. Kim, C.-H. Park, Introduction and nutritional evaluation of buckwheat sprouts as a new vegetable, Food Res. Int. 37 (4) (2004) 319–327.
[8] C.-L. Liu, Y.-S. Chen, J.-H. Yang, B.-H. Chiang, Antioxidant activity of tartary (*Fagopyrum tataricum* (L.) Gaertn.) and common (*Fagopyrum esculentum* Moench) buckwheat sprouts, J. Agric. Food Chem. 56 (1) (2007) 173–178.
[9] O. Laila, I. Murtaza, Seed sprouting: a way to health promoting treasure, Int. J. Curr. Res. Rev. 6 (23) (2014) 70–74.
[10] S. Jain, U.K. Patil, Phytochemical and pharmacological profile of *Cassia tora* Linn.-an overview, Indian J. Nat. Prod. Resour. 1 (2010) 430–437.

[11] T.-F. Tzeng, H.-J. Lu, S.-S. Liou, C.J. Chang, I.-M. Liu, *Cassia tora* (Leguminosae) seed extract alleviates high-fat diet-induced nonalcoholic fatty liver, Food Chem. Toxicol. 51 (2013) 194–201.
[12] S.-M. Wong, M.M. Wong, O. Seligmann, H. Wagner, New antihepatotoxic naphthopyrone glycosides from the seeds of *Cassia tora*, Planta Med. 55 (03) (1989) 276–280.
[13] D.S. Jang, G.Y. Lee, Y.S. Kim, Y.M. Lee, C.-S. Kim, J.L. Yoo, J.S. Kim, Anthraquinones from the seeds of *Cassia tora* with inhibitory activity on protein glycation and aldose reductase, Biol. Pharm. Bull. 30 (11) (2007) 2207–2210.
[14] J.-M. Cherng, W. Chiang, J.-H. Wang, C.-M. Lin, C.-Y. Lee, C.-M. Shih, L.-C. Chiang, Anthraquinones of edible wild vegetable *Cassia tora* stimulate proliferation of human $CD4^+$ T lymphocytes and secretion of interferon-gamma or interleukin 10, Food Chem. 107 (4) (2008) 1576–1580.
[15] X. Dong, J. Fu, X. Yin, C. Yang, X. Zhang, W. Wang, X. Du, Q. Wang, J. Ni, Cassiae semen: a review of its phytochemistry and pharmacology, Mol. Med. Report. 16 (3) (2017) 2331–2346.
[16] J. Kwon, H. Lee, Y.H. Seo, J. Yun, J. Lee, H.C. Kwon, Y. Guo, J.S. Kang, J.-J. Kim, D. Lee, Cytotoxic drimane sesquiterpenoids isolated from *Perenniporia maackiae*, J. Nat. Prod. (2018).
[17] T. Bruhn, A. Schaumlöffel, Y. Hemberger, G. Bringmann, Specdis: quantifying the comparison of calculated and experimental electronic circular dichroism spectra, Chirality 25 (4) (2013) 243–249.
[18] K. Zhu, H. Zhou, H. Qian, Antioxidant and free radical-scavenging activities of wheat germ protein hydrolysates (WGPH) prepared with alcalase, Process Biochem. 41 (6) (2006) 1296–1302.
[19] S.-H. Lee, S.-C. Ko, S.-M. Kang, S.H. Cha, G.-N. Ahn, B.-H. Um, Y.-J. Jeon, Antioxidative effect of *Ecklonia cava* dried by far infrared radiation drying, Food Sci. Biotechnol. 19 (1) (2010) 129–135.
[20] S. Kitanaka, M. Takido, Studies on the constituents of the seeds of *Cassia obtusifolia*: the structures of two new lactones, isotoralactone and cassialactone, Phytochemistry 20 (8) (1981) 1951–1953.
[21] S. Kitanaka, M. Takido, Studies on the constituents of the seeds of *Cassia obtusifolia* L. the structures of two naphthopyrone glycosides, Chem. Pharm. Bull. 36 (10) (1988) 3980–3984.
[22] G. Alemayehu, B. Abegaz, G. Snatzke, H. Duddeck, Bianthrones from *Senna longiracemosa*, Phytochemistry 32 (5) (1993) 1273–1277.
[23] S. Kitanaka, M. Takido, Studies on the constituents of the roots of *Cassia torosa*. II. the structures of two dimeric tetrahydroanthracenes, Chem. Pharm. Bull. 38 (5) (1990) 1292–1294.
[24] Z.-W. Wang, J.-S. Wang, J. Luo, D.-D. Wei, L.-Y. Kong, Three new phenolic glucosides from the roots of *Rheum palmatum*, Chem. Pharm. Bull. 60 (2) (2012) 241–245.
[25] S. Shrestha, P. Paudel, S.H. Seong, B.S. Min, E.K. Seo, H.A. Jung, J.S. Choi, Two new naphthalenic lactone glycosides from *Cassia obtusifolia* L. seeds, Arch. Pharm. Res. 41 (2018) 737–742.
[26] G.Y. Lee, D.S. Jang, Y.M. Lee, J.M. Kim, J.S. Kim, Naphthopyrone glucosides from the seeds of *Cassia tora* with inhibitory activity on advanced glycation end products (AGEs) formation, Arch. Pharm. Res. 29 (7) (2006) 587–590.
[27] J.-W. Shen, J.-S. Jiang, X.-F. Zhang, C.-F. Zheng, P.-C. Zhang, Two new benzochromone glycosides from the stem of *Berchemia racemosa*, J. Asian Nat. Prod. Res. 9 (6) (2007) 499–503.
[28] F. Liu, F.-S. Li, Z.-M. Feng, Y.-N. Yang, J.-S. Jiang, L. Li, P.-C. Zhang, Neuroprotective naphthalene and flavan derivatives from *Polygonum cuspidatum*, Phytochemistry 110 (2015) 150–159.
[29] R. Mei, H. Liang, J. Wang, L. Zeng, Q. Lu, Y. Cheng, New *seco*-anthraquinone glucosides from *Rumex nepalensis*, Planta Med. 75 (10) (2009) 1162–1164.
[30] S.G. Wubshet, I.M. Brighente, R. Moaddel, D. Staerk, Magnetic ligand fishing as a targeting tool for HPLC-HRMS-SPE-NMR: α-glucosidase inhibitory ligands and alkylresorcinol glycosides from *Eugenia catharinae*, J. Nat. Prod. 78 (11) (2015) 2657–2665.
[31] Q. Mei, C. Wang, W. Yuan, G. Zhang, Selective methylation of kaempferol via benzylation and deacetylation of kaempferol acetates, Beilstein J. Org. Chem. 11 (2015) 288–293.
[32] K. Yamauchi, T. Mitsunaga, M. Inagaki, T. Suzuki, Synthesized quercetin derivatives stimulate melanogenesis in B16 melanoma cells by influencing the expression of melanin biosynthesis proteins MITF and p38 MAPK, Bioorg. Med. Chem. 22 (13) (2014) 3331–3340.
[33] K. Kazuma, N. Noda, M. Suzuki, Malonylated flavonol glycosides from the petals of *Clitoria ternatea*, Phytochemistry 62 (2) (2003) 229–237.
[34] Y. Ding, C. Liang, H.T. Nguyen, E.-M. Choi, J.-A. Kim, Y.-H. Kim, Chemical constituents from *Acer mandshuricum* and their effects on the function of osteoblastic MC3T3-E1 cells, Bull. Korean Chem. Soc. 31 (4) (2010) 929–933.
[35] H. Nakano, K.K. Schrader, L.K. Mamonov, T.S. Kustova, V.K. Mursaliyeva, C. L. Cantrell, Isolation and identification of *Flavobacterium columnare* and *Streptococcus iniae* antibacterial compounds from the terrestrial plant *Atraphaxis laetevirens*, J. Agric. Food Chem. 60 (42) (2012) 10415–10419.
[36] S. Kitanaka, M. Takido, Studies on the constituents of the seeds of *Cassia obtusifolia* Linn. the structures of three new anthraquinones, Chem. Pharm. Bull. 32 (3) (1984) 860–864.
[37] L. Du, T. Zhu, H. Liu, Y. Fang, W. Zhu, Q. Gu, Cytotoxic polyketides from a marine-derived fungus *Aspergillus glaucus*, J. Nat. Prod. 71 (11) (2008) 1837–1842.
[38] Y.-S. Kil, S.M. Kim, U. Kang, H.Y. Chung, E.K. Seo, Peroxynitrite-scavenging glycosides from the stem bark of *Catalpa ovata*, J. Nat. Prod. 80 (8) (2017) 2240–2251.
[39] M.J. Kim, D.-C. Kim, J. Kwon, S.M. Ryu, H. Kwon, Y. Guo, S.-B. Hong, Y.-C. Kim, H. Oh, D. Lee, Anti-inflammatory metabolites from *Chaetomium nigricolor*, J. Nat. Prod. 83 (4) (2020) 881–887.
[40] Y. Son, Y.-K. Cheong, N.-H. Kim, H.-T. Chung, D.G. Kang, H.-O. Pae, Mitogen-activated protein kinases and reactive oxygen species: how can ROS activate MAPK pathways? J. Signal Transduction 2011 (2011) 1–6.